Borneo Journal of Pharmacy
Vol 8 Issue 2 May 2025
Pages 176 – 183

https://journal.umpr.ac.id/index.php/bjop/article/view/9574
DOI: https://doi.org/10.33084/bjop.v8i2.9574
e-ISSN: 2621-4814

Research Article

Molecular Docking Study of *Illicium verum* Hook f. as Elastase and Collagenase Inhibitor in Anti-aging Mechanism

Ave Rahman [1]

Tri Widiandani [2]

Retno Widyowati [2,3,4*]

[1] Master Program of Pharmaceutical Science, Universitas Airlangga, Surabaya, East Java, Indonesia
[2] Department of Pharmaceutical Sciences, Universitas Airlangga, Surabaya, East Java, Indonesia
[3] Natural Product Drug Discovery & Development Research Group, Universitas Airlangga, Surabaya, East Java, Indonesia
[4] Skin and Cosmetic Technology Centre of Excellence, Universitas Airlangga, Surabaya, East Java, Indonesia

*email: rr-retno-w@ff.unair.ac.id; phone: +6281615886978

Keywords:
Anti-aging
Collagenase
Elastase
Illicium verum
Molecular docking

Abstract

Skin aging, a natural physiological process intensified by external factors that augment the activity of aging-related enzymes such as elastase and collagenase, leads to the degradation of collagen solubility and the disruption of elastin fiber cross-linking. This study aimed to investigate the potential of secondary metabolites from *Illicium verum* fruit as inhibitors of both elastase and collagenase through an *in silico* molecular docking approach. The methodology involved ligand and protein preparation, validation of the docking protocol, the molecular docking simulation itself, and subsequent visualization of amino acid residue interactions. The protein targets utilized were elastase (PDB ID: 1Y93) and collagenase (PDB ID: 2D1N). The docking results identified gingerol as exhibiting the highest binding affinity for elastase (-7.99 kcal/mol), followed by carvacrol (-6.79 kcal/mol) and ferulic acid (-6.24 kcal/mol). Similarly, for collagenase, gingerol displayed the strongest interaction (-8.47 kcal/mol), followed by carvacrol (-6.30 kcal/mol) and α-pinene (-6.24 kcal/mol). Notably, gingerol and carvacrol also demonstrated favorable amino acid similarity scores and promising interactions within the active sites of both elastase and collagenase. In conclusion, this molecular docking study suggests that the secondary metabolites of *I. verum* fruit possess potential anti-aging activity by inhibiting elastase and collagenase enzymes.

Received: March 29th, 2025
1st Revised: April 10th, 2025
Accepted: May 8th, 2025
Published: May 30th, 2025

INTRODUCTION

Aging is an inevitable physiological process that affects all living organisms, including humans, manifesting visibly in the skin and systemically in various organs[1]. The skin, as the body's largest organ, is particularly susceptible to environmental damage, accelerating its aging process. Structurally, the skin comprises three distinct layers. The outermost layer, the epidermis, is primarily composed of keratinocyte cells, vital for keratin synthesis, and melanocyte cells, responsible for skin pigmentation[2,3]. Beneath the epidermis lies the dermis, a complex connective tissue system rich in fibroblasts, collagen, and elastin fibers[4]. This layer, which constitutes the bulk of the skin, is crucial for its flexibility, elasticity, and tensile strength[2,5]. The deepest layer, the subcutaneous connective tissue, consists of fat cell lobules and plays a significant role in hormone regulation[3].

Skin aging can be broadly categorized into chronological (intrinsic) aging, driven by internal biological factors, and photoaging (extrinsic aging), which results from external aggressors. Chronological aging leads to a gradual reduction in the skin's physiological function over time, while external factors such as ultraviolet (UV) radiation, chemical exposure, poor nutrition, and lifestyle choices significantly exacerbate skin damage[6,7]. This multifaceted aging process induces profound changes in skin biology and structure. Key alterations include reductions in skin thickness and water content, altered collagen solubility, and increased cross-linking of collagen and elastin fibers. Clinically, these changes manifest as increased

How to cite: Rahman A, Widiandani T, Widyowati RR. Molecular Docking Study of Illicium verum Hook f. as Elastase and Collagenase Inhibitor in Anti-aging Mechanism. Borneo J Pharm. 2025;8(2):176-83. doi:10.33084/bjop.v8i2.9574

skin laxity and fragility, the appearance of fine lines, and the disruption of elastin networks[4,8]. Mechanistically, collagen damage is often mediated by elevated collagenase activity, while elastase activity directly impacts the integrity and cross-linking of elastin fibers. An increase in the activity of these two enzymes is a critical factor in accelerating the skin aging process[9,10].

Given the profound impact of oxidative stress and inflammation on skin aging, natural compounds with antioxidant and anti-inflammatory properties are of significant interest for dermatological applications. *Illicium verum* Hook f., commonly known as star anise, is widely recognized for its use in cosmetic products, where it functions as a perfuming material, skin conditioner, tonic, and soothing agent, as listed in the Cosmetic Ingredients database of the European Commission[11]. Beyond its cosmetic applications, *I. verum* fruit is also well-documented for its potent anti-inflammatory, antibacterial, and antioxidant activities[12,13]. These properties are directly relevant to the intricate mechanisms of skin aging, as oxidative stress is a primary driver, with reactive oxygen species (ROS) promoting collagen degradation and diminishing skin elasticity[14]. Furthermore, inflammatory mediators upregulate matrix metalloproteinases (MMPs), particularly collagenase (MMP-1), which actively degrade collagen within the skin's extracellular matrix[15]. The observed bioactivities of *I. verum* fruit are largely attributed to its rich composition of phenolic compounds, including rutin, ferulic acid, caffeic acid, gallic acid, and catechin[16]. Despite its traditional use and promising phytochemical profile, studies specifically investigating the anti-aging activity of *I. verum* fruit have not been previously reported. Therefore, in this study, we employed molecular docking simulations to investigate the interaction of secondary metabolites from *I. verum* ethanolic extract with collagenase and elastase enzymes, aiming to elucidate its potential anti-aging mechanisms.

MATERIALS AND METHODS

Materials

This study utilized secondary metabolites derived from *I. verum*, specifically those identified in its essential oil and ethanol extract. The key compounds investigated included carvacrol, limonene, camphene, α-pinene, gingerol, ferulic acid, rutin, methyl anisate, and kojic acid[17]. The chemical structures of these compounds were retrieved from the PubChem database (https://pubchem.ncbi.nlm.nih.gov/). For enzyme structures, collagenase (PDB ID: 2D1N) and elastase (PDB ID: 1Y93) were obtained from the Protein Data Bank (https://www.rcsb.org/), complete with their respective bound ligands.

Molecular docking simulations were performed using AutoDockTools, which facilitated macromolecule preparation and the execution of docking protocols. Specifically, autogrid4.exe and autodock4.exe were employed for grid generation and docking operations, respectively. Avogadro software was utilized for the energy minimization of ligands prior to docking. For the visualization and analysis of ligand-receptor interactions, BIOVIA Discovery Studio Visualizer 2024 v.24.1.0.23298 was used. All computational tasks were conducted on an Acer Aspire A514-54G laptop, featuring an 11th Gen Intel® Core™ i3-1115G4 processor clocked at 3.00 GHz, 8.00 GB of RAM, and running a 64-bit operating system.

Methods

Protein preparation

Protein structures of collagenase and elastase were prepared using AutoDockTools for subsequent molecular docking simulations. For collagenase, chain A from the Collagenase-3 (MMP-13) complexed with a hydroxamic acid inhibitor was utilized, possessing a protein resolution of 2.37 Å. Meanwhile, elastase preparation involved chain A from the crystal structure of the catalytic domain of human MMP12, complexed with acetohydroxamic acid, resolved at an exceptional 1.03 Å atomic resolution. Prior to docking, all water molecules and non-standard residues were meticulously removed from both protein structures. Subsequently, hydrogen atoms and Kollman charges were added to ensure proper chemical representation. The prepared protein structures were then saved in .pdbqt format, ready for the molecular docking procedures[18].

Ligand preparation

The specific compounds from *I. verum* extract utilized in this study were identified through prior LC-MS/MS profiling conducted by our research group in a separate investigation[17]. These identified compounds include carvacrol, thymol, limonene, camphene, α-pinene, gingerol, ferulic acid, rutin, and methyl anisate. For molecular docking simulations, the 3D

structures of these compounds were retrieved in *.sdf format from the PubChem database. To ensure the most stable conformation for docking, the energy of each compound was subsequently minimized using the "Optimize Geometry" tool within Avogadro software. The optimized structures were then saved in *.pdb format.

Further preparation for docking was performed using AutoDockTools. Each minimized ligand in *.pdb format was opened via the "Input Ligand" menu. The ligands were then prepared for docking by defining their rotatable bonds using the "Torsion Tree" tools. This involved a series of steps: "detect root," "choose root," "set number of torsion," and "choose torsion." Finally, the prepared ligands were saved in .pdbqt format, ready for subsequent docking analyses[18].

Method validation

The reliability and accuracy of the molecular docking simulations were ensured through a rigorous method validation process. This involved re-docking the native ligand back into the active site of each target protein. For this procedure, AutoDockTools was utilized to define a grid box (40 x 40 x 40 points) precisely centered on the known native ligand position within the protein's binding pocket. Specifically, for protein 1Y93, the re-docking was performed with the grid box centered at coordinates x: 1.632, y: -1.803, and z: 4.393, and a grid spacing of 0.142 Å. For protein 2D1N, the grid box was centered at x: -44.048, y: 25.846, and z: -19.485, with a grid spacing of 0.375 Å.

A critical metric for successful validation is the Root Mean Square Deviation (RMSD) value. An RMSD value of less than 2.0 Å signifies that the re-docked ligand's predicted pose is sufficiently close to its experimentally determined native conformation, thus confirming the docking method's ability to accurately reproduce the optimal ligand binding position[19]. To confirm this accuracy, the native ligands of each protein, elastase (acetohydroxamic acid) and collagenase (*N*-[(2R)-6-amino-1-(hydroxyamino)-1-oxohexan-2-yl]-10-[2-[(diaminomethylideneamino)methyl]phenyl]decanamide), were re-docked, and their respective RMSD values were verified to be below the 2.0 Å threshold.

Molecular docking

Molecular docking simulations were performed using AutoDockTools to evaluate the binding affinity and molecular interactions of star anise compounds with the 1Y93 and 2D1N receptors. The energy of binding was expressed in kcal/mol. Crucially, the grid box size and coordinates for each receptor were maintained consistently with those established during the validation process, ensuring comparability and reliability of the docking results.

Data analysis

Ligand-receptor interactions were meticulously evaluated based on two primary criteria: the similarity of amino acid residues involved in the binding site and the specific types of interactions formed between the ligands (both native and tested compounds) and the receptor[20]. This comparative analysis allowed for a comprehensive assessment of how effectively the compounds mimicked or modulated the binding characteristics of the native ligand.

RESULTS AND DISCUSSION

The molecular docking protocol employed in this study was rigorously validated to ensure its reliability. For the 1Y93 receptor, the RMSD between the docked and experimental ligand conformations was 1.83 ± 0.02 Å. Similarly, for the 2D1N receptor, the RMSD was 1.16 ± 0.07 Å. These low RMSD values confirm the accuracy and applicability of our docking methodology for evaluating ligand-receptor interactions[21].

Our investigation into the secondary metabolites of *I. verum* extract revealed their potential as inhibitors of 1Y93 and 2D1N through molecular docking simulations. Notably, gingerol exhibited the strongest binding affinity to 1Y93, achieving a docking score of -8.85 ± 0.36 kcal/mol. This score significantly surpassed those of both the positive control, kojic acid (-3.53 ± 0.02 kcal/mol), and the native ligand (-3.09 ± 0.01 kcal/mol). Other promising compounds, carvacrol and ferulic acid, also demonstrated favorable receptor binding with docking scores of -6.79 ± 0.01 kcal/mol and -6.23 ± 0.01 kcal/mol, respectively. Similarly, molecular docking results for *I. verum* secondary metabolites against 2D1N indicated substantial inhibitory potential, often surpassing that of the reference compound, kojic acid (−4.27 ± 0.02 kcal/mol). Gingerol again emerged as a leading inhibitor, achieving the highest docking score of −8.12 ± 0.49 kcal/mol, followed by carvacrol (−6.35 ± 0.07 kcal/mol) and α-pinene (−6.24 ± 0.01 kcal/mol) (**Table I**).

Table I. Molecular docking scores and inhibition constants of secondary metabolites of *I. verum* on 1Y93 and 2D1N (average ± SD).

Ligands	1Y93		2D1N	
	Docking score (ΔG; kcal/mol)	Inhibition constant (Ki; µM)	Docking score (ΔG; kcal/mol)	Inhibition constant (Ki; µM)
Native ligand	-3.09 ± 0.01	545 ± 1.73	-9.96 ± 0.01	0.49 ± 0.02
Carvacrol	-6.79 ± 0.01	10.5 ± 0.07	-6.35 ± 0.07	22.21 ± 2.5
Limonene	-6.22 ± 0.03	27.44 ± 1.59	-5.93 ± 0.01	44.22 ± 0.03
Camphene	-5.70 ± 0.04	67 ± 4.59	-5.98 ± 0.01	41.31 ± 0.15
α-pinene	-5.95 ± 0.01	43.57 ± 1.27	-6.24 ± 0.01	26.33 ± 0.57
Gingerol	-8.85 ± 0.36	0.7 ± 0.61	-8.12 ± 0.49	1.31 ± 0.98
Ferulic acid	-6.23 ± 0.01	27.09 ± 0.76	-5.27 ± 0.01	138.76 ± 0.76
Rutin	-5.99 ± 0.86	73.18 ± 83.01	-5.10 ± 0,07	183.06 ± 21.09
Methyl anisate	-6.13 ± 0.03	32.17 ± 1.42	-5.46 ± 0,01	100.63 ± 0.7
Kojic acid	-3.53 ± 0.02	2.56 ± 0.08	-4.27 ± 0.02	741.64 ± 21.61

Further analysis of gingerol's interaction with 1Y93 (**Table II**) showed a high amino acid similarity score of 60.00% with Ala182, His218, and Glu219, indicating shared critical binding residues with the native ligand. The interaction similarity score between gingerol and the native ligand was 40.00%, primarily involving hydrogen bonds at Ala182 and Glu219, alongside van der Waals interactions at His218. Interestingly, gingerol formed a higher number of hydrogen bonds at the 1Y93 binding site compared to other tested ligands, specifically at five sites: Ala182, Glu219, Leu181, Ala234, and Thr239. This increased number of hydrogen bonds likely contributes to gingerol's superior docking score, as such interactions are known to strengthen molecular binding affinity[22]. In contrast, carvacrol and ferulic acid displayed lower amino acid similarity scores of 20.00% (His218) and 40.00% (Ala182, His218), respectively. The detailed interaction between the elastase receptor and gingerol, carvacrol, as well as ferulic acid is visually represented in **Figure 1**.

Table II. Drug-compound interactions (amino acid residues and interaction types) and native ligand similarity scores of 1Y93.

Parameter	Native ligand	Carvacrol	Limonene	Camphene	α-pinene	Gingerol	Ferulic acid	Rutin	Methyl anisate
Amino acid residue	His228[e]	-	-	-	-	-	-	-	-
	Ala182[a]	-	-	-	-	-	-	-	-
	His218[a]	-	Ala182[b]	-	-	Ala182[a]	Ala182[ab]	Ala182[a]	-
	His222[a]	His218[b]	His218[b]	His218[bc]	His218[bc]	His218[b]	His218[be]	His218[a]	His218[b]
	Glu219[af]	-	-	-	-	-	-	His222[a]	-
	-	-	-	-	-	Glu219[a]	-	-	Glu219[a]
	-	Thr239[e]	Leu181[b]	Leu181[b]	Leu181[b]	Leu181[a]	Leu181[abc]	Leu181[a]	Leu181[b]
	-	Tyr240[b]	-	Tyr240[b]	Tyr240[b]	Tyr240[b]	Tyr240[a]	-	Tyr240[b]
	-	Val235[a]	-	-	-	Val235[ae]	Val235[a]	-	-
	-	-	-	-	-	His228[b]	-	-	-
	-	-	-	-	-	Ile180[b]	-	-	-
	-	-	-	-	-	Ala234[a]	-	-	-
	-	-	-	-	-	Thr239[a]	-	-	-
	-	-	-	-	-	-	Gly179[a]	-	-
	-	-	-	-	-	-	Lys241[a]	-	Lys241[a]
	-	-	-	-	-	-	-	Ala184[a]	-
	-	Phe237[a]	-	-	-	-	-	His183[b]	-
	-	-	-	-	-	-	-	His172[a]	-
Similarity of amino acid with native ligand (%)		20	40	20	20	60	40	60	40
Similarity of interaction with the native ligand (%)		0	0	0	0	40	20	60	20
Similarity in ligand-receptor interaction (%)*		10	20	10	10	50	30	60	30

Note: [a]hydrogen bond, [b]alkyl/pi-alkyl, [c]pi-sigma, [d]pi-cation, [e]unfavorable donor-donor, [f]attractive charge, *(similarity of amino acid + similarity type of interaction)/2

Gingerol demonstrated an amino acid similarity score of 40.00% with the native ligand of 2D1N, similar to rutin, and shared common binding sites including Thr245, Ile243, Ala186, His222, Val219, and Leu239 (**Table III**). The interaction profile of gingerol exhibited a 33.33% similarity with the native ligand, forming hydrogen bonds at Thr245, Ile243, Ala186, and His222, and van der Waals interactions at Val219 and Leu239. Furthermore, gingerol formed the most numerous hydrogen bonds among the tested ligands within the 2D1N binding site, engaging seven residues: Thr245, Ile243, Ala186, His222, Leu185, Gly183, and Phe241. This extensive hydrogen bonding network, similar to that observed with the 1Y93, correlates with

gingerol's superior docking score. The interactions between the collagenase receptor and gingerol, carvacrol, as well as α-pinene are visually presented in **Figure 2**.

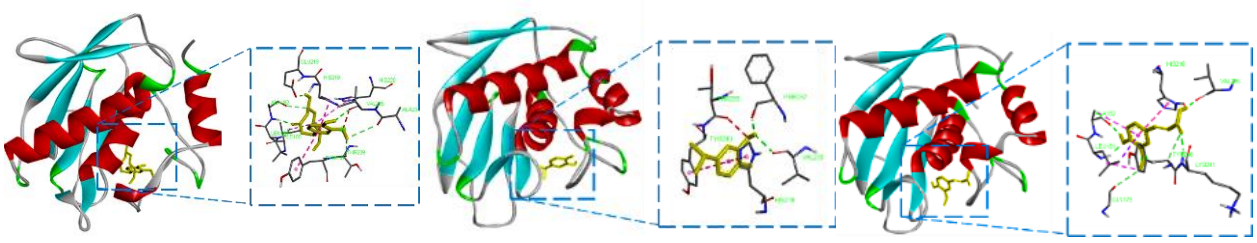

a b c

Figure 1. Ligand interactions of compounds with the best docking scores against the 1Y93 receptor: (**a**) gingerol, (**b**) carvacrol, and (**c**) ferulic acid.

Table III. Drug-compound interactions (amino acid residues and interaction types) and native ligand similarity scores of 2D1N.

Parameter	Native ligand	Carvacrol	Limonene	Camphene	α-pinene	Gingerol	Ferulic acid	Rutin	Methyl anisate
Amino acid residue	Ala238[a]	-	-	-	-	-	-	-	-
	Thr245[a]	Thr245[a]	-	-	-	Thr245[a]	Thr245[a]	-	Thr245[a]
	Ile243[a]	-	-	-	-	Ile243[a]	Ile243[a]	-	-
	Pro236[a]	-	-	-	-	-	-	-	-
	Ala188[a]	-	-	-	-	-	-	-	-
	Glu223[a]	-	-	-	-	-	-	Glu223[a]	-
	His226[a]	-	-	-	-	-	-	His226[a]	-
	Ala186[a]	-	-	-	-	Ala186[a]	Ala186[ab]	Ala186[a]	-
	His232[a]	-	-	-	-	-	-	His232[a]	His232[b]
	His222[a]	-	His222[b]	His222[b]	His222[bc]	His222[ad]	His222[d]	His222[a]	His222[bc]
	Val219[b]	-	-	-	-	-	-	-	-
	Tyr244[b]	-	Val219[b]	-	Val219[b]	Val219[b]	Val219[b]	-	Val219[b]
	Leu218[b]	Tyr244[c]	Tyr244[b]	-	Tyr244[b]	-	-	Tyr244[a]	-
	Leu239[bc]	-	-	-	-	-	-	-	-
	-	-	-	Leu239[b]	-	Leu239[b]	-	-	-
	-	-	Leu185[b]	-	-	Leu185[ab]	Leu185[abc]	Leu185[a]	-
	-	-	-	-	-	Gly183[a]	-	Gly183[a]	-
	-	-	-	-	-	Phe241[ab]	-	Phe241[a]	-
	-	-	-	-	-	-	-	Pro242[b]	-
Similarity of amino acid with native ligand (%)		13.33	20	13.33	20	40	33.33	40	26.67
Similarity of interaction with the native ligand (%)		6.67	13.33	0	13.33	33.33	26.67	40	13.33
Similarity in ligand-receptor interaction (%)*		10	16.67	6.67	16.67	36.67	30	40	20

Note: [a]hydrogen bond, [b]alkyl/pi-alkyl, [c]pi-sigma, [d]pi-cation, [e]unfavorable donor-donor, [f]attractive charge, *(similarity of amino acid + similarity type of interaction)/2

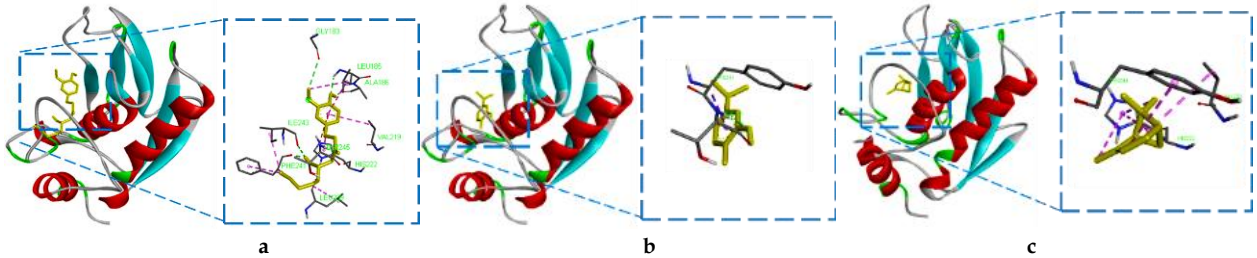

a b c

Figure 2. Ligand interactions of compounds with the best docking scores against the 2D1N receptor: (**a**) gingerol, (**b**) carvacrol, and (**c**) α-pinene.

Plant extracts are complex mixtures of metabolites, where not all compounds may contribute equally to pharmacological activity. Nonetheless, many are classified as bioactive compounds capable of synergistic, additive, or even antagonistic effects[23]. Major classes of metabolites recognized for their medicinal properties, such as alkaloids, terpenoids, and phenolic compounds, often exhibit anti-inflammatory or antimicrobial activities[24]. However, the intricate composition of extracts, typically comprising hundreds of metabolites, complicates the identification of specific activity for individual compounds, classifying plant extracts as multi-target interaction agents[23]. Elevated levels of free radicals, originating from both internal

metabolic processes and external environmental factors, can significantly upregulate the activity of collagenase and elastase. This, in turn, leads to the degradation of the extracellular matrix (ECM), which is primarily composed of vital structural proteins like collagen, elastin, and hyaluronic acid[25].

Gingerol, a prominent phenolic compound identified in *I. verum* extract, is widely recognized as a key active component in *Zingiber officinale*, contributing to its established anti-inflammatory and antioxidant properties. Both *Z. officinale* and *I. verum* share the presence of gingerol, which imparts the characteristic pungent flavor. Gingerol's anti-aging effects have been linked to its capacity for oxidative stress reduction. It has been shown to enhance the activity of crucial antioxidant enzymes, including superoxide dismutase (SOD), catalase (CAT), and glutathione peroxidase (GPx), as well as elevating glutathione (GSH) levels in various animal models[26]. Both MMP-13 and MMP-12 are crucial macromolecular targets belonging to the MMPs family[27]. These enzymes play a pivotal role in the degradation of the collagen matrix, directly influencing skin elasticity, strength, and flexibility[1]. Specifically, MMP-13 and MMP-12 are responsible for cleaving various types of collagen (I, II, III, IV) and elastin, respectively[27]. The anti-collagenase and anti-elastase activities of gingerol have been substantiated in several studies. For instance, *Z. officinale* extract, rich in gingerol, has been demonstrated to inhibit the activity of various MMPs, including MMP-1, MMP-3, and MMP-13, in human synovial fibroblast models[28]. Given that MMPs are central to tissue degradation processes associated with aging, their inhibition is a crucial strategy for mitigating systemic aging effects and for the development of cosmeceutical products.

CONCLUSION

This study provides compelling evidence, based on molecular docking simulations, that secondary metabolites within *I. verum* fruit extract exhibit promising anti-aging activity through the inhibition of collagenase and elastase enzymes. Specifically, gingerol and carvacrol demonstrated high potential as future anti-aging agents, characterized by favorable molecular docking scores, significant amino acid similarity, and robust binding interactions. To validate these *in silico* predictions and confirm the observed enzymatic inhibition, future research should prioritize direct *in vitro* enzymatic assays for collagenase and elastase using *I. verum* extract.

ACKNOWLEDGMENT

This research was generously supported by the Ministry of Education, Culture, Research, and Technology, Republic of Indonesia, under contract numbers 040/E5/PG.02.00.PL/2024 and 1683/B/UN3.LPPM/PT.01.03/2024.

AUTHORS' CONTRIBUTION

Conceptualization: Ave Rahman, Tri Widiandani, Retno Widyowati
Data curation: Ave Rahman
Formal analysis: Ave Rahman, Tri Widiandani, Retno Widyowati
Funding acquisition: Retno Widyowati
Investigation: Ave Rahman, Tri Widiandani, Retno Widyowati
Methodology: Ave Rahman, Tri Widiandani, Retno Widyowati
Project administration: Ave Rahman
Resources: Ave Rahman, Retno Widyowati
Software: Ave Rahman, Tri Widiandani
Supervision: Tri Widiandani, Retno Widyowati
Validation: Ave Rahman, Tri Widiandani, Retno Widyowati
Visualization: Ave Rahman, Tri Widiandani, Retno Widyowati
Writing - original draft: Ave Rahman
Writing - review & editing: Ave Rahman, Tri Widiandani, Retno Widyowati

DATA AVAILABILITY

The structural data analyzed in this study are publicly available and can be accessed through the RCSB PDB and PubChem.

CONFLICT OF INTEREST

The authors declare no conflicts of interest related to this study.

REFERENCES

1. Elgamal AM, El Raey MA, Gaara A, Abdelfattah MAO, Sobeh M. Phytochemical profiling and anti-aging activities of Euphorbia retusa extract: In silico and in vitro studies. Arab J Chem. 2021;14(6):103159. DOI: 10.1016/j.arabjc.2021.103159

2. Agrawal R, Hu A, Bollag WB. The Skin and Inflamm-Aging. Biology. 2023;12(11):1396. DOI: 10.3390/biology12111396; PMCID: PMC10669244; PMID: 37997995

3. James WD, Berger TG, Elston DM. Andrews' Diseases of the Skin: Clinical dermatology. 12th edition. Philadelphia: Elsevier Saunders; 2016.

4. Soheilifar MH, Masoudi-Khoram N, Shirkavand A, Ghorbanifar S. Non-coding RNAs in photoaging-related mechanisms: a new paradigm in skin health. Biogerontology. 2022;23(3):289–306. DOI: 10.1007/s10522-022-09966-x; PMID: 35587318

5. Chu DH. Overview of biology, development, and structure of skin. In: Wolff K, Goldsmith LA, Katz SI, Gilchrest BA, Paller AS, Leffell DJ, editors. Fitzpatrick's dermatology in general medicine. 7th edition. New York: McGraw-Hill; 2008. p. 57–73.

6. Nurrochmad A, Wirasti W, Dirman A, Lukitaningsih E, Rahmawati A, Fakhrudin N. Effects of Antioxidant, Anti-Collagenase, Anti-Elastase, Anti-Tyrosinase of The Extract and Fraction from Turbinaria decurrens Bory. Indones J Pharm. 2018;29(4):188-99. DOI: 10.14499/indonesianjpharm29iss4pp188

7. Papaccio F, Arino AD, Caputo S, Bellei B. Focus on the Contribution of Oxidative Stress in Skin Aging. Antioxidants. 2022;11(6):1121. DOI: 10.3390/antiox11061121; PMCID: PMC9220264; PMID: 35740018

8. Park S. Biochemical, Structural and Physical Changes in Aging Human Skin, and Their Relationship. Biogerontology. 2022;23(3):275–88. DOI: 10.1007/s10522-022-09959-w; PMCID: PMC10316705; PMID: 35292918

9. Guo L, Qi J, Du D, Liu Y, Jiang X. Current advances of Dendrobium officinale polysaccharides in dermatology: a literature review. Pharm Biol. 2020;58(1):664–73. DOI: 10.1080/13880209.2020.1787470; PMCID: PMC7470034; PMID: 32657196

10. Birkedal-Hansen H. Catabolism and turnover of collagens: collagenases. Methods Enzymol. 1987;144:140-71. DOI: 10.1016/0076-6879(87)44177-3; PMID: 3041177

11. Sharafan M, Jafernik K, Ekiert H, Kubica P, Kocjan R, Blicharska E, et al. Illicium verum (Star Anise) and Trans-Anethole as Valuable Raw Materials for Medicinal and Cosmetic Applications. Molecules. 2022;27(3):650. DOI: 10.3390/molecules27030650; PMCID: PMC8839413; PMID: 35163914

12. Lin CY, Kao SH, Hung LC, Chien HJ, Wang WH, Chang YW, et al. Lipopolysaccharide-Induced Nitric Oxide and Prostaglandin E2 Production Is Inhibited by Tellimagrandin II in Mouse and Human Macrophages. Life. 2021;11(5):411. DOI: 10.3390/life11050411; PMCID: PMC8146495; PMID: 33946374

13. Luís Â, Sousa S, Wackerlig J, Dobusch D, Duarte AP, Pereira L, et al. Star anise (Illicium verum Hook. f.) essential oil: Antioxidant properties and antibacterial activity against Acinetobacter baumannii. Flavour Fragr J. 2019;34(4):260–70. DOI: 10.1002/ffj.3498

14. Lee JH, Park J, Shin DW. The Molecular Mechanism of Polyphenols with Anti-Aging Activity in Aged Human Dermal Fibroblasts. Molecules. 2022;27(14):4351. DOI: 10.3390/molecules27144351; PMCID: PMC9322955; PMID: 35889225

15. Jiratchayamaethasakul C, Ding Y, Hwang O, Im ST, Jang Y, Myung SW, et al. In vitro screening of elastase, collagenase, hyaluronidase, and tyrosinase inhibitory and antioxidant activities of 22 halophyte plant extracts for novel cosmeceuticals. Fish Aquatic Sci. 2020;23:6. DOI: 10.1186/s41240-020-00149-8

16. Aly SE, Sabry BA, Shaheen MS, Hathout AS. Assessment of antimycotoxigenic and antioxidant activity of star anise (Illicium verum) in vitro. J Saudi Soc Agric Sci. 2016;15(1):20–7. DOI: 10.1016/j.jssas.2014.05.003

17. Noumi E, Ahmad I, Adnan M, Patel H, Merghni A, Haddaji N, et al. Illicium verum L. (Star Anise) Essential Oil: GC/MS Profile, Molecular Docking Study, In Silico ADME Profiling, Quorum Sensing, and Biofilm-Inhibiting Effect on Foodborne Bacteria. Molecules. 2023;28(23):7691. DOI: 10.3390/molecules28237691; PMCID: PMC10707387; PMID: 38067422

18. Pratama MRF, Poerwono H, Siswodihardjo S. Molecular docking of novel 5-O-benzoylpinostrobin derivatives as wild type and L858R/T790M/V948R mutant EGFR inhibitor. J Basic Clin Physiol Pharmacol. 2019;30(6): 2019-0301. DOI: 10.1515/jbcpp-2019-0301; PMID: 31855568

19. Hevener KE, Zhao W, Ball DM, Babaoglu K, Qi J, White SW, et al. Validation of Molecular Docking Programs for Virtual Screening against Dihydropteroate Synthase. J Chem Inf Model. 2009;49(2):444–60. DOI: 10.1021/ci800293n; PMCID: PMC2788795; PMID: 19434845

20. Pratama MRF, Poerwono H, Siswodihardjo S. Introducing a two‐dimensional graph of docking score difference vs. similarity of ligand‐receptor interactions. Indones J Biotechnol. 2021;26(1):54-60. DOI: 10.22146/ijbiotech.62194

21. Pratama RR, Sholikhah I, Sukardiman S, Sahu RK, Widyowati R. Phytochemical Compounds Identification From 70% Ethanol Extract of Arcangelesia Flava (L.) Merr Stems Using LC-MS/MS and In-Silico Molecular Docking Approach as Inhibitor Interleukin-1β. Pharmacogn J. 2023;15(4):528–34. DOI: 10.5530/pj.2023.15.114

22. Chen D, Oezguen N, Urvil P, Ferguson C, Dann SM, Savidge TC. Regulation of protein-ligand binding affinity by hydrogen bond pairing. Sci Adv. 2016;2(3):e1501240. DOI: 10.1126/sciadv.1501240; PMCID: PMC4820369; PMID: 27051863

23. Vaou N, Stavropoulou E, Voidarou C (Chrysa), Tsakris Z, Rozos G, Tsigalou C, et al. Interactions between Medical Plant-Derived Bioactive Compounds: Focus on Antimicrobial Combination Effects. Antibiotics. 2022;11(8):1014. DOI: 10.3390/antibiotics11081014; PMCID: PMC9404952; PMID: 36009883

24. Wink M. Modes of Action of Herbal Medicines and Plant Secondary Metabolites. Medicines. 2015;2(3):251–86. DOI: 10.3390/medicines2030251; PMCID: PMC5456217; PMID: 28930211

25. Abdelfattah MAO, Dmirieh M, Bakrim WB, Mouhtady O, Ghareeb MA, Wink M, et al. Antioxidant and anti-aging effects of Warburgia salutaris bark aqueous extract: Evidences from in silico, in vitro and in vivo studies. J Ethnopharmacol. 2022;292:115187. DOI: 10.1016/j.jep.2022.115187

26. Ayustaningwarno F, Anjani G, Ayu AM, Fogliano V. A critical review of Ginger's (Zingiber officinale) antioxidant, anti-inflammatory, and immunomodulatory activities. Front Nutr. 2024;11:1364836. DOI: 10.3389/fnut.2024.1364836; PMCID: PMC11187345; PMID: 38903613

27. Alipour H, Raz A, Zakeri S, Djadid ND. Therapeutic applications of collagenase (metalloproteases): A review. Asian Pac J Trop Biomed. 2016;6(11):975–81. DOI: 10.1016/j.apjtb.2016.07.017

28. Hwang JH, Jung HW, Oh SY, Kang JS, Kim JP, Park YK. Effects of Zingiber officinale extract on collagen-induced arthritis in mice and IL-1β-induced inflammation in human synovial fibroblasts. Eur J Inflamm. 2017;15(3):168–78. DOI: 10.1177/1721727X17727997